

Article

Experimental Investigation of Unsteady Pressure Pulsation in New Type Dishwasher Pump with Special Double-Tongue Volute

Yilei Zhu ¹, Jinfeng Zhang ¹, Yalin Li ^{1,2,*}, Ping Huang ¹, Hui Xu ² and Feng Zheng ²

¹ National Research Center of Pumps, Jiangsu University, Zhenjiang 212013, China; 2211811038@stmail.ujs.edu.cn (Y.Z.); zhangjinfeng@ujs.edu.cn (J.Z.); huangping@ujs.edu.cn (P.H.)

² Ningbo FOTILE Kitchen Ware Co., Ltd., Ningbo 315336, China; xuh@fotile.com (H.X.); zhengfeng@fotile.com (F.Z.)

* Correspondence: ylli@ujs.edu.cn

Abstract: A pressure pulsation experiment of a dishwasher pump with a passive rotation double-tongue volute was carried out and compared with the pressure pulsation of a single-tongue volute and a static double-tongue volute. The pressure pulsation of the three volute models was compared and analyzed from two aspects of different impeller speeds and different monitoring points. The frequency domain and time–frequency domain of pressure pulsation were obtained by a Fourier transform and short-time Fourier transform, respectively. The results showed that the average pressure of each monitoring point on the rotating double-tongue volute was the smallest and that on the single-tongue volute was the largest. When the impeller rotates at 3000 rpm, there were eight peaks and valleys in the pressure pulsation time domain curve of the single-tongue volute, while the double-tongue volute was twice that of the single-tongue volute. Under different impeller speeds, the changing trends of pressure pulsation time and frequency domain curves of static and rotating double-tongue volutes at monitoring point p1 are basically the same. Therefore, a volute reference scheme with passive rotation speed is proposed in this study, which can effectively improve the flow pattern and reduce pressure inside the dishwasher pump, and also provide a new idea for rotor–rotor interference to guide the innovation of dishwashers.

Keywords: dishwasher pump; pressure pulsation; rotor–rotor interaction; impeller speeds; double-tongue volute; experiment



Citation: Zhu, Y.; Zhang, J.; Li, Y.; Huang, P.; Xu, H.; Zheng, F. Experimental Investigation of Unsteady Pressure Pulsation in New Type Dishwasher Pump with Special Double-Tongue Volute. *Machines* **2021**, *9*, 288. <https://doi.org/10.3390/machines9110288>

Academic Editor: Dan Zhang

Received: 25 October 2021

Accepted: 11 November 2021

Published: 14 November 2021

Publisher's Note: MDPI stays neutral with regard to jurisdictional claims in published maps and institutional affiliations.



Copyright: © 2021 by the authors. Licensee MDPI, Basel, Switzerland. This article is an open access article distributed under the terms and conditions of the Creative Commons Attribution (CC BY) license (<https://creativecommons.org/licenses/by/4.0/>).

1. Introduction

Today, dishwashers are used by more and more families. Compared with manual dishwashing, a dishwasher can not only shorten the cleaning time but also save water and labor, making dishwashing simple. Therefore, domestic and foreign companies have launched various models of dishwasher to meet the market, for example, the DWA5—1513 dishwasher from TOSHIBA, the SC73M12TI dishwasher from SIMENS, the NP-8LZK5RX dishwasher from Panasonic, and the RX600 dishwasher from Midea, etc. What these dishwashers have in common is that they perform the cleaning function through the passive rotation of the built-in spray arm. The dishwasher pump system is an important part of the dishwasher system, which can complete the water transport and spraying function. This paper is based on FOTILE company dishwasher pump system research. The dishwasher of this company is accepted by many people because it can achieve open cleaning without pipelines. The pipeline-free cleaning replaces the pipeline with a double-tongue volute flow channel that can be passively rotated. The symmetrical design of the volute is conducive to its rotation, and the jet hole is set on the volute spray arm to realize the function of water spraying. This avoids the problem of fouling and is more convenient for daily cleaning and maintenance. Of course, the nozzle structure, injection angle, and jet velocity will affect the cleaning effect [1,2]. However, the pressure pulsation during the operation of the dishwasher pump will cause the vibration of the dishwasher, which

will reduce the stability of the system and reduce the service life [3–5]. Dishwashers are household appliances accompanied by pressure pulsation noise, which seriously affects the user experience.

An important part of the pump system is the volute structure and parameters (volute tongue angle, cross-section shapes, volute differ shape, etc.). It will affect the pump performance and internal flow [6,7]. In recent years, scholars have studied many volute structures and volute parameter optimization to improve pump performance and reduce unstable flow. Jin et al. [8] studied the influence of the gap between the volute tongue and the impeller on the pressure pulsation and the performance of the double suction pump. Results suggested that as the gap increased, the value of the head and the pressure pulsation were reduced, and the efficiency was increased. Alemi et al. [9] considered the parameters (cutwater gap, tongue shape, and volute tongue angle) of a centrifugal pump. The research found that the best volute tongue angle is 5° , which lets the radial force be lower 40% than others at the design point. Patil et al. [10] investigated four volute tongue clearances of 6%, 8%, 10%, and 12.5% of impeller diameter in the centrifugal blower and found that the volute tongues' clearance decreases from 12.5% to 6% of impeller diameter, and the total pressure and efficiency increase by 19.52% and 21.90%, respectively, in a full discharge condition. Shim et al. [11] carried out multi-objective optimization for the double-volute centrifugal pump with a diaphragm, and the pressure pulsation of the optimized model was significantly reduced. Yang et al. [12] studied four parameters of the volute of centrifugal pump. It was found that the volute designed with a round cross-section shape and the volute spiral development areas designed according to the constant swirl can achieve high efficiency. A large volute throat area could obtain smooth pump performance, and the optimal radial gap between the impeller and the volute tongue is 15 mm.

Scholars use a numerical simulation and experimental test as the main methods to study the pressure pulsation in the pump. Usually, test methods are used to validate the accuracy of simulations [13–16]. Li et al. [17] completed numerical analysis on the reduction of pressure pulsation for a double-section centrifugal pump and proposed that a combination of multi-blades, a larger radial gap, and staggering arrangements can reduce the pressure pulsation inside the pump. Zhang et al. [18] explored the pressure pulsation in a nuclear reactor coolant pump. It was confirmed that pressure pulsation acting on the impeller's blade is mainly dominated by the impeller rotating frequency, the vane passing frequency, and the double blade-passing frequency, and the pressure pulsation acting on the blade's pressure surface is more intense than on the suction surface. Tan et al. [19] completed numerical analysis of the blade rotational angle on the pressure pulsation of a mixed-flow pump and proved that the main frequency of pressure pulsation in the impeller was dominated by shaft frequency or blade frequency. Meng et al. [20] found that the peak efficiency of the runner with splitter blades in an ultra-high head turbine is higher than that of the impeller without splitter blades. Xia et al. [21] explained that the rotating stall of the impeller leads to rotor–dynamic instabilities and causes strong vibrations when the pump-turbine is in pump mode. Wu et al. [22] investigated the pressure pulsation in a centrifugal pump by experiment. The results showed that an unstable separation vortex in the impeller flow passages causes the frequency to be located in the range from 100 to 145 Hz. Shi et al. [23] studied the pressure pulsation characteristics in a full tubular pump under different flow conditions and found that the dominant frequency of the pressure pulsation decreases as the flow rate increases. Zhang et al. [24] found that the rotor–stator interface-induced component of the vaneless area pressure pulsation can be effectively decreased by enlarging the vaneless area. Song et al. [25] performed an experimental investigation of pressure pulsation in an axial flow pump. The results showed that the floor-attached vortex can induce a low-frequency pulsation of 2.12 Hz, which let the amplitudes of pressure pulsation be larger than those without the floor-attached vortex.

At present, the research on the pressure pulsation in the pump is mostly based on the static condition of the volute, and the research on the pressure pulsation under the passive rotation of the volute is still rare. Therefore, in order to reveal the new 'rotor–rotor'

interference mechanism between the high-speed rotation of the impeller and the low-speed passive rotation of the volute, this paper studies the pressure pulsation characteristics of the double-tongue volute under passive rotation at different impeller speeds through an innovative rotating pressure test device. In addition, the pressure pulsation characteristics of the single-tongue volute and the double-tongue volute at rest are compared and studied, which provides a reference for the design and optimization of the open pump.

2. Open Test Rig Setup for Dishwasher Pump

As shown in Figure 1, the open test setup of the dishwasher pump was set at the National Research Center of Pumps, Jiangsu University. The test rig was inside a transparent water tank in order to observe the working state of the dishwasher more conveniently, and the tank is $400 \times 440 \times 400$ mm. The shaft of the motor at the bottom of the water tank connects the impeller to control the operation of the dishwasher pump.

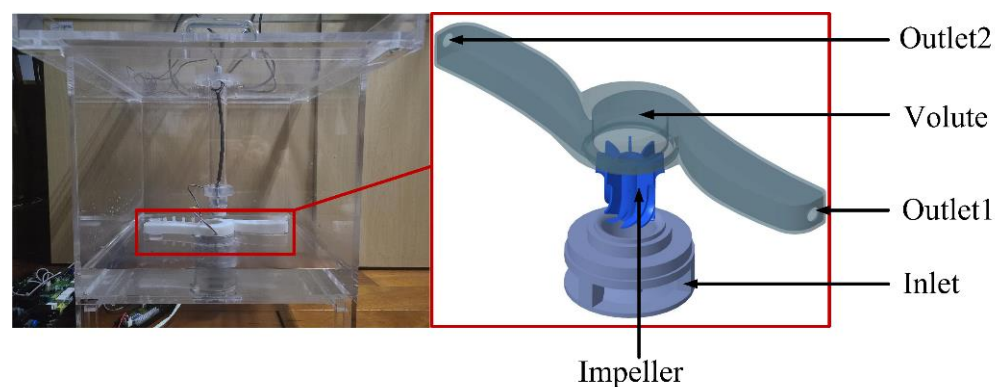


Figure 1. Open test rig of the dishwasher pump.

The dishwasher pump consists of a compound impeller with eight blades and a spray arm of the volute type. The bottom end of the compound impeller is a forward-curved axial flow blade, the top is a radial centrifugal blade, and there is no obvious front shroud and back shroud. The volute had two symmetrical flow channels that helped the spray arm rotate. In particular, an unsealed connection between the impeller and the volute is also designed to enhance the cleaning effect of the dishwasher by passively rotating the spray arm. The specific design parameters of the dishwasher pump are shown in Figure 2 and listed in Table 1. The flow rate Q and head H under design point were 55 L/min and 2 m, respectively. The impeller speed n was designed as 3000 rpm.

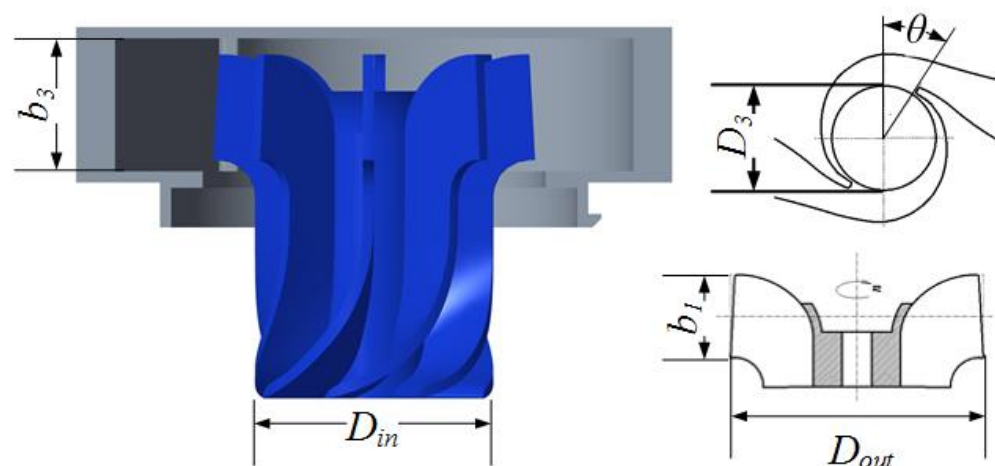


Figure 2. Dimension labeling of dishwasher pump.

Table 1. Essential parameters of the dishwasher pump.

	Parameter	Value
Impeller	Impeller inlet diameter D_{in} (mm)	32
	Impeller outlet width b_1 (mm)	14.15
	Impeller outlet diameter D_{out} (mm)	43.3
	Number of blades Z	8
Volute	Volute inlet width b_3 (mm)	17.8
	Volute base circle diameter D_3 (mm)	46
	Volute tongue angle θ ($^\circ$)	34

3. Experimental Tests

Figure 3 shows a schematic diagram of data acquisition and the transient pressure test setting of the dishwasher pump. The whole test system consists of two parts. The first system was to change the speed of the impeller. By adjusting the speed control button on the panel, the panel will feedback a number. One hundred times, the number is the rotating speed of the impeller, and the unit is rpm. The second system was to measure the transient pressures of the dishwasher pump. The pressure pulsation sensors (SCYG314) produced by Senno Sci-tech Co., Ltd. were supported by a 15 V DC power source. The accuracy of each pressure sensor was 0.2%, and the range of measurement was 0–20 kpa. The sensors were connected to the data acquisition unit by a converter, and the computer accepted the converted current signal by a data line. The test software of pressure pulsation is smart and integrates functions that can change the sampling time and frequency. In order to ensure the accuracy of the test, there was zero calibration of the sensor before the formal test. The sampling frequency f_s was set at 10,000 Hz, and the data were acquired for 2 s when the dishwasher pump reached a stable condition. The sampling frequency is much larger than blade frequency and satisfies Shannon's sampling law [26–29]. In addition, in order to solve the problem of the pressure pulsation test in the process of volute rotation, the rotating pressure pulsation test device was designed. The top of the device is bolted to the cover of the water tank, and the sensor probe extending from the bottom of the device is placed in a preset monitoring hole on the volute. The part of the device near the sensor probe can be rotated by the electricity slip ring, which can not only ensure the normal electricity consumption of the sensor but also effectively avoid the wire winding problem in the rotation test process. The whole device was waterproofed to ensure the normal operation of the sensor.

In order to verify that the test repeatability could be reliable, repeated multiple measurements for the pressure pulsation of monitoring point p1 were carried out. According to the obtained data, the time domain curves of the pressure pulsation of the three tests are drawn, as shown in Figure 4a, and they are periodic distribution in the time of the impeller rotating for two cycles, and the curve trend is basically the same. It is clearly shown that the maximum deviation of average pressure is 1.9% from Figure 4b.

The positions of pressure pulsation monitoring points of the volute of the dishwasher pump are shown in Figure 5. The pressure monitoring point p1 is on the side of the volute, and it is positive in the impeller outlet direction. The pressure monitoring points p2, p3, p4, p5, and p6 were distributed in the top of the volute, and in turn, it extends from the tongue position of the volute to the outlet of the volute.

To investigate the influence of the impeller speeds on the pressure pulsation in the dishwasher pump, five different speeds of the impeller were modified by the impeller speed control system, which was previously mentioned in Figure 3. As shown in Figure 6, in order to further study the influence of the volute form and the passive rotation of the volute on the pressure pulsation, the pressure pulsation tests were carried out on the single-tongue volute and the double-tongue volute at rest and compared with the double-tongue volute rotation model. In order to make the comparative test more scientific and rigorous, each pressure pulsation monitoring point position of three different volute models was consistent during the test.

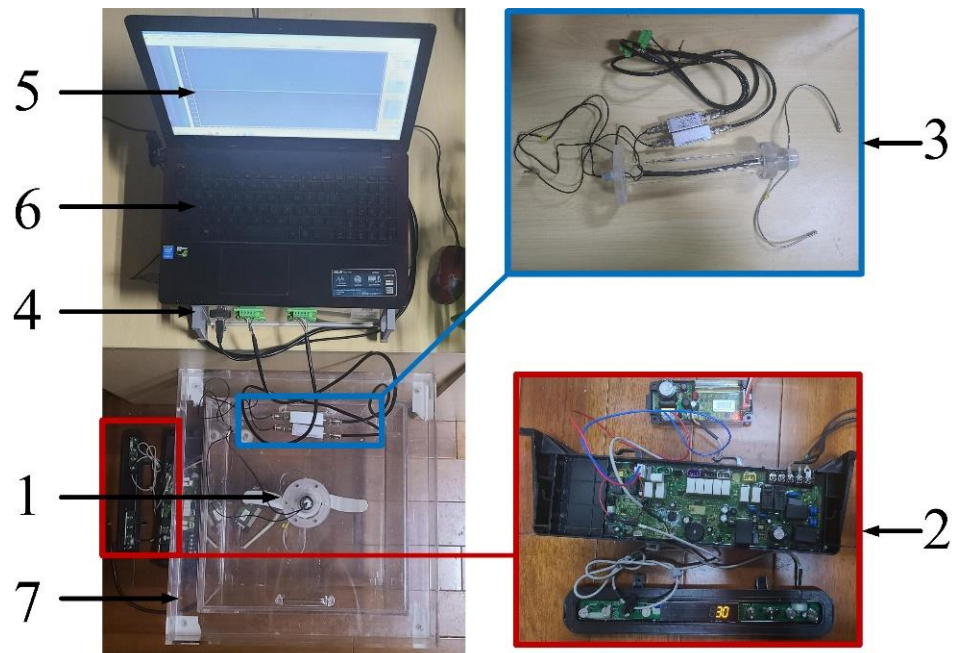
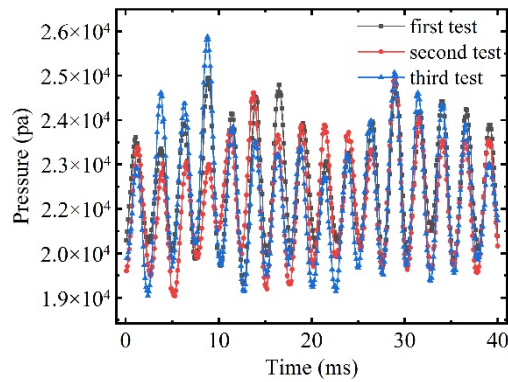
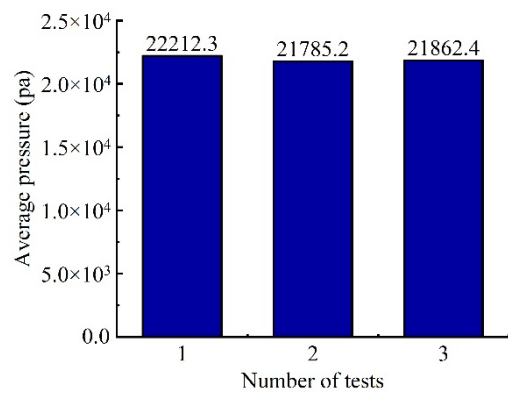


Figure 3. Dishwasher pump test system. 1: dishwasher pump, 2: impeller speed regulator, 3: rotating pressure pulsation test device, 4: data-acquisition system, 5: software interface, 6: personal computer, and 7: water tank.



(a)



(b)

Figure 4. Three pressure pulsation tests. (a) Pressure pulsation curves at three tests; (b) comparison of average pressure at three tests.

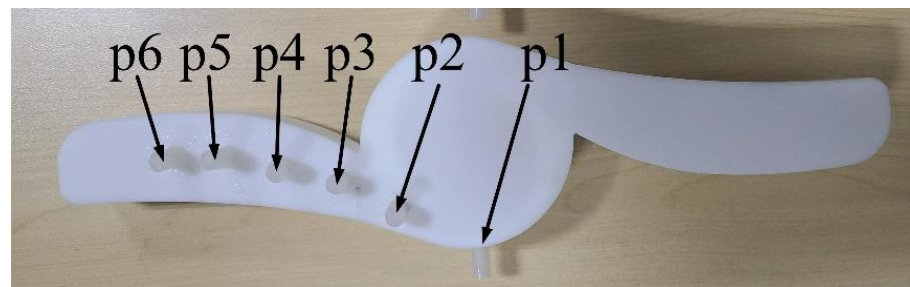


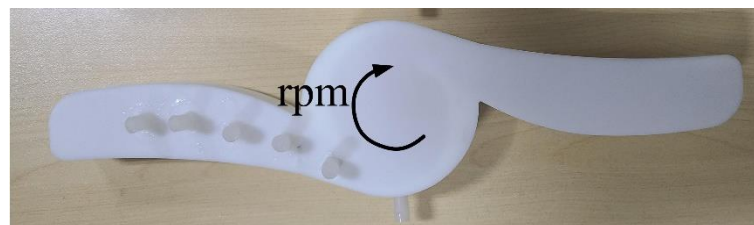
Figure 5. Pressure pulsation monitoring points positions.



(a)



(b)



(c)

Figure 6. Tested volutes. (a) single-tongue volute; (b) double-tongue volute (static); (c) double-tongue volute (rotate).

4. Result and Discussion

To facilitate the normalization of pressure pulsation data, the time–frequency analysis method was introduced to describe the pressure pulsation. The method of time–frequency can not only give the frequency of the pressure pulsation but also show the information about the frequency domain representation changes with time. This method is using a short-time Fourier transform (STFT) to transform the time domain signal of pressure pulsation [30–32]. The source signal is divided into several small signal segments by the window function. Firstly, the signal of each segment is converted to one-dimensional by Fourier transform, and then the two-dimensional time–frequency diagram is obtained by the translation of the window function.

$$S_x(t, f) = \int_t [x(t) \times w(t - t')] \times e^{-j2\pi ft} dt \quad (1)$$

where $x(t)$ is the source signal, and $w(t - t')$ is the window function. The window function is Hanning.

4.1. Pressure Pulsation Analysis with Different Volutes

4.1.1. Time–Frequency Domain Analysis of Pressure Pulsation

Figure 7 shows the time–frequency domain of pressure pulsation for three volutes at six different monitoring positions. It shows the dynamic pressure pulsation is unsteady and dependent on time. The main frequency of pressure pulsation of the single-tongue volute is 1 times blade frequency, while the main frequency of pressure pulsation of the double-tongue volute is 2 times blade frequency, and the secondary frequency is 1 times blade frequency, indicating that the static and dynamic interference is the root cause of pressure pulsation. The amplitude pulsation of pressure pulsation of the double-tongue volute at 1000 Hz is also strong at monitoring points p1, p2, and p6. Compared with the stationary double-tongue volute, the amplitude of the double-blade frequency of the rotating double-tongue volute will reach a maximum between 400 and 1200 ms, which is higher than the amplitude of the main frequency at other times (Figure 7i,l). This is probably caused by the new dynamic interference between the volute and the rotating impeller, which is also used as a rotating component.

4.1.2. Comparative Analysis of Pressure Fluctuation Average Pressure

Figure 8 shows a comparison of the average pressure at different pressure pulsation monitoring points when the dishwasher pump with three different types of volute. It can be seen that the average pressure of the single-tongue volute is the largest at the monitoring point p4, while that of the double-tongue volute reaches the maximum at the monitoring point p3. In three different volute models, the average pressure of each monitoring point is the largest at the same impeller speed due to the minimum flow passage of the single-tongue volute. Similarly, in the process of passive rotation, the double-tongue volute can effectively alleviate the squeezing effect of water flow on the volute, making the average pressure minimum. The variation trend of average pressure of three volute models from p1 to p3 at the monitoring point is the same. However, the change of the rotating double-tongue volute from p3 to p6 at the monitoring points is more smooth, and the maximum deviation of the average pressure is 1.4%. The maximum deviations of average pressure of the single-tongue volute and static double-tongue volute are 4.5% and 4.9%, respectively. This is because when the double-tongue volute rotates, the flow pattern in the volute channel is improved, and the pressure distribution is uniform.

4.1.3. Dominant Frequency Amplitudes of the Pressure Pulsation

The dominant frequency amplitudes of the pressure pulsation for three volutes at different measuring points are shown in Figure 9. On the double-tongue volute, the amplitude of dominant frequency of the pressure pulsation increases first and then decreases from p1 to p6 at the monitoring point and reaches the maximum at the monitoring point p2. The amplitude of dominant frequency of pressure pulsation at different monitoring points of the single-tongue volute has no obvious regularity, and the amplitude of p1 reaches the maximum at the monitoring point. This is because the experiment is carried out at the impeller speed of 3000 rpm, which is much higher than the design speed of the single-tongue volute. The leakage vortex at the outlet of the impeller disturbs the flow field around the monitoring point p1, changes the stable structure of the flow field at the outlet of the impeller, and leads to severe pressure pulsation in the flow field. The larger impeller speed increases the flow velocity in the vortex chamber and deteriorates the flow pattern, which is the reason for the irregular amplitude of the dominant frequency of the pressure pulsation in the single-tongue volute.

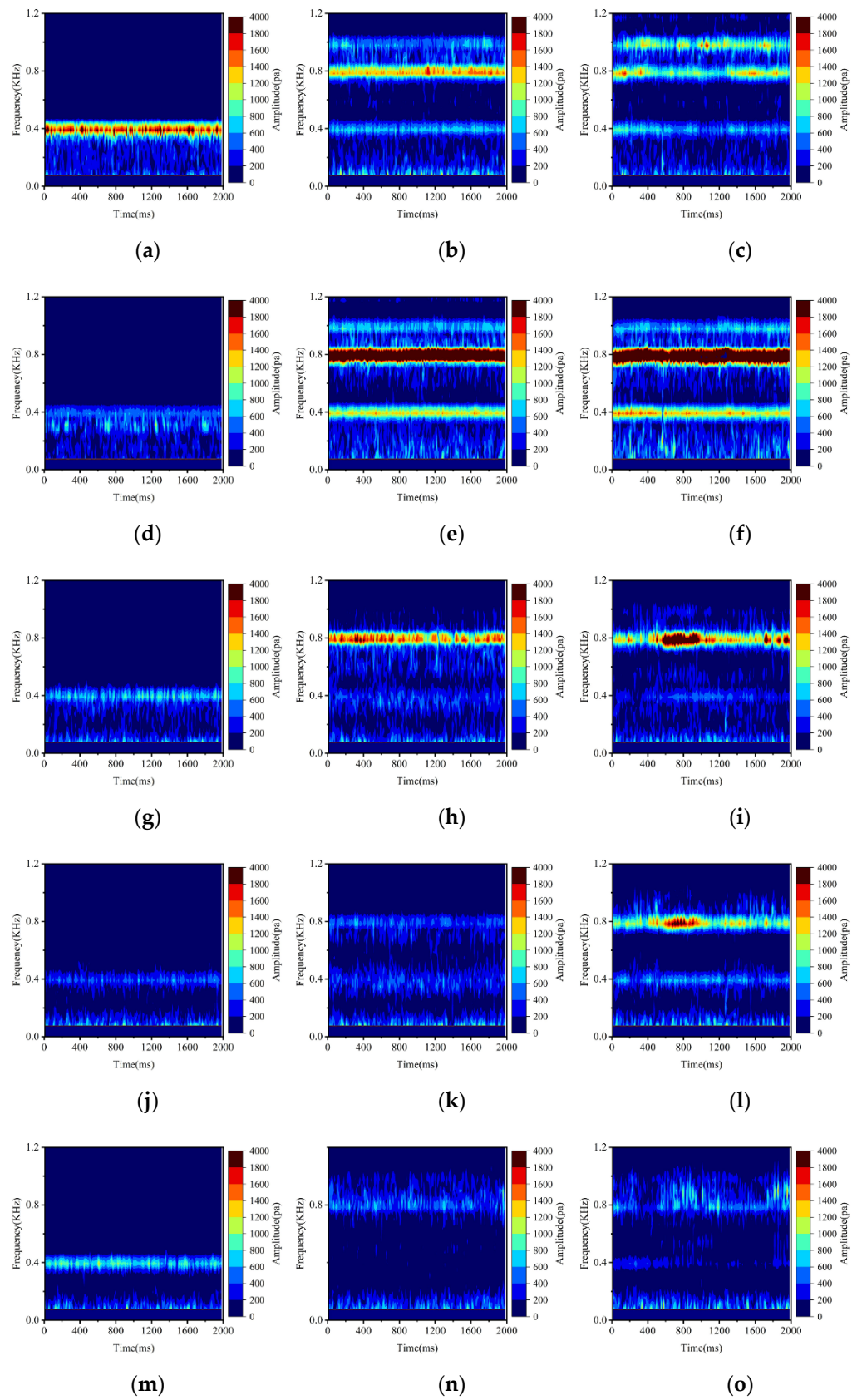


Figure 7. Cont.

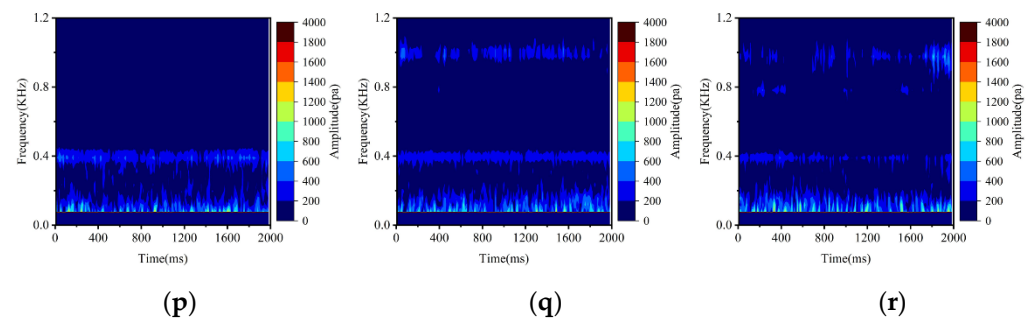


Figure 7. Time–frequency domain of pressure pulsation for three volutes at different positions. (a) p1 at single-tongue volute; (b) p1 at double-tongue volute (static); (c) p1 at double-tongue volute (rotate); (d) p2 at single-tongue volute; (e) p2 at double-tongue volute (static); (f) p2 at double-tongue volute (rotate); (g) p3 at single-tongue volute; (h) p3 at double-tongue volute (static); (i) p3 at double-tongue volute (rotate); (j) p4 at single-tongue volute; (k) p4 at double-tongue volute (static); (l) p4 at double-tongue volute (rotate); (m) p5 at single-tongue volute; (n) p5 at double-tongue volute (static); (o) p5 at double-tongue volute (rotate); (p) p6 at single-tongue volute; (q) p6 at double-tongue volute (static); (r) p6 at double-tongue volute (rotate).

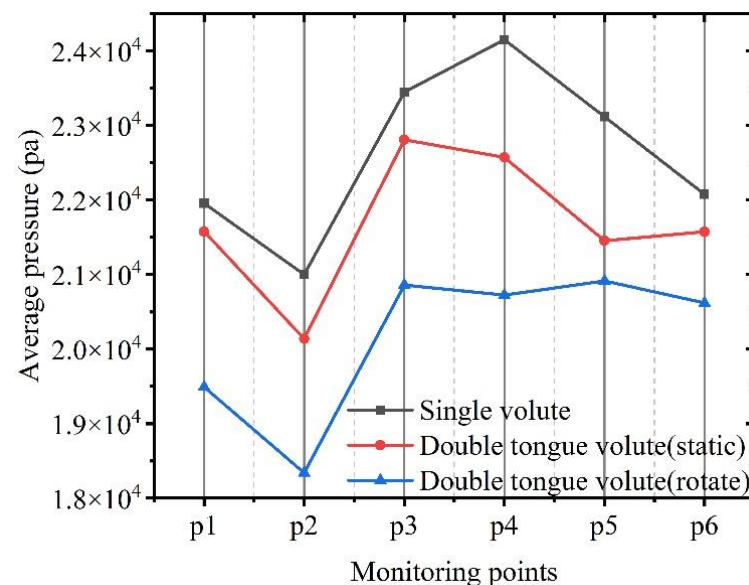


Figure 8. The variation trend of average pressure with different volutes.

4.2. Pressure Pulsation Analysis at Different Impeller Speeds

4.2.1. Time–Domain Analysis of Pressure Fluctuation

Pressure pulsation appears when the rotating impeller blades sweep through the tongue of the volute. Apparently, the number of blades skimming over the volute tongue and the structure of the volute play an important role in the change of pressure pulsation. Figure 10 shows the time domain variation of pressure pulsation at p1 for three volutes at different impeller speeds. With the decrease of impeller speeds, the pressure peak value and the amplitudes of pressure pulsation decrease. When the impeller rotates at 3000, 2500, and 2000 rpm, the variations of pressure pulsation with different volutes all have certain periodicity. When the impeller rotates at 1500 and 1000 rpm, the variations of pressure pulsation with different volutes all have certain periodicity, the pressure fluctuates violently, and the pressure distribution is uneven. This is because, at low rotational speeds, the pressure and flow rate of the blade acting on the flow will decrease, which keeps air in the pump chamber. The coupling of water and air makes the flow field in the dishwasher pump more complex, and the flow pattern becomes unstable, which lets the time domain curve of pressure pulsation be uneven.

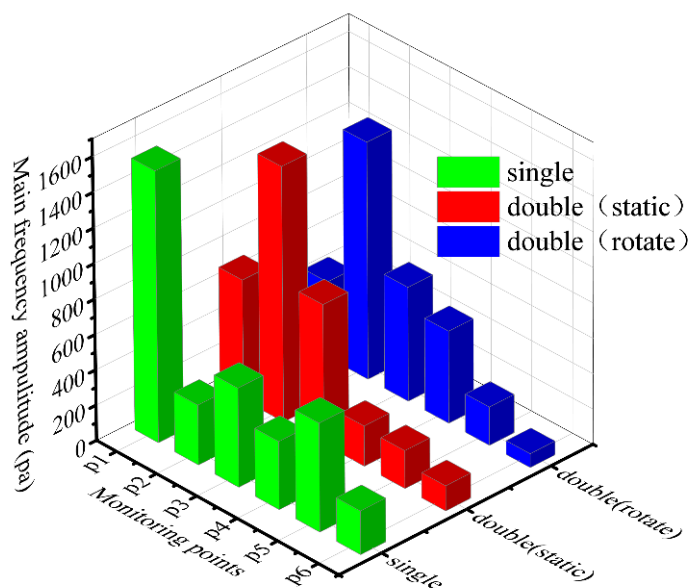


Figure 9. Dominant frequency amplitudes of pressure pulsation for three volutes at different measuring points.

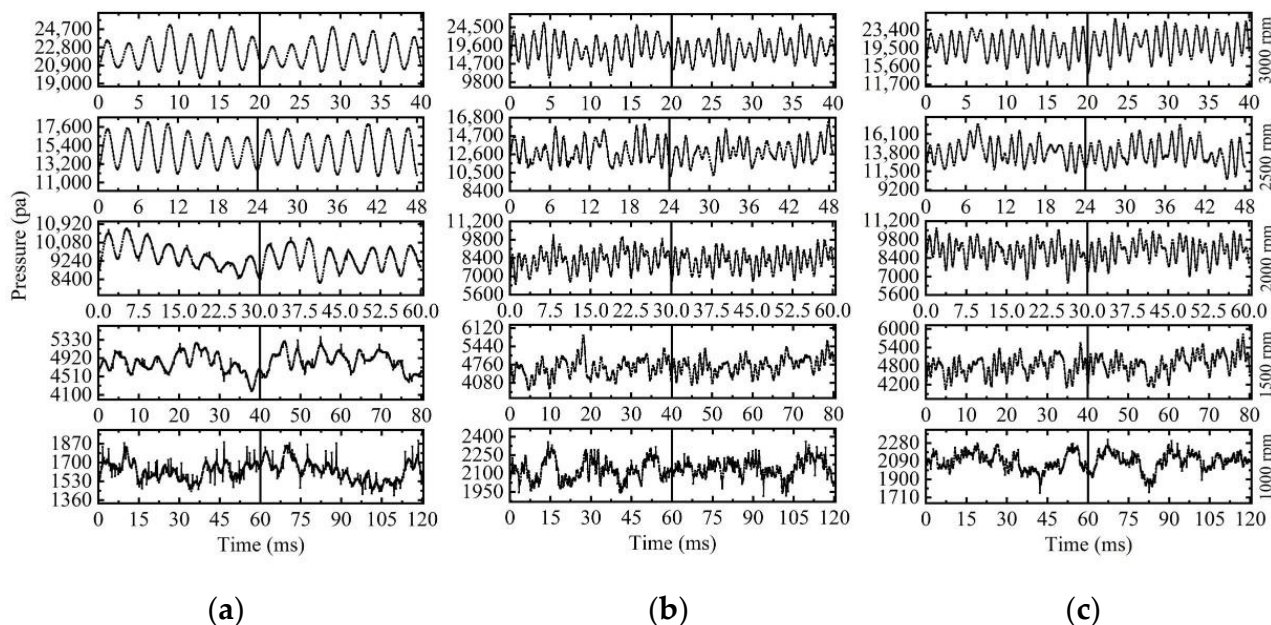


Figure 10. Time domain of pressure pulsation for three volutes at different impeller speeds. (a) Single-tongue volute; (b) double-tongue volute (static); (c) double-tongue volute (rotate).

As shown in Figure 10a, the curves of pressure pulsation have eight peaks and troughs when the impeller rotates at 3000, 2500, and 2000 rpm, and the dishwasher pump has a single-tongue volute. The number of cycles corresponds to the number of blades [33–35]. In addition, from Figure 10b,c, it is apparent that the curves of pressure pulsation have 16 peaks and troughs when the pump has a double-tongue volute and the impeller is 3000 and 2500 rpm. It is the same as the number of volute tongues multiplied by the number of blades. It is explained that the rotor–stator interference between the impeller and volute is the fundamental cause of pressure pulsation. Compared with the pump double-tongue volute under static and rotating conditions, the amplitudes of pressure pulsation of the pump with static volute are significantly higher than those of the pump with a rotating volute at different impeller speeds.

4.2.2. Frequency–Domain Analysis of Pressure Fluctuation

The shaft frequency (f_n) and blade frequency (f_{BPF}) of the pump are determined by the rotational speeds of the impeller (n), and blade frequency depends on the axial frequency and blade number. Equation (2) lists the relationship between the f_n (kHz), f_{BPF} (kHz) and n (rpm) [36–38].

$$\begin{aligned} f_n &= 1/\frac{60}{n} \\ f_{BPF} &= 8f_n \end{aligned} \quad (2)$$

The calculated parameters of the pump at different impeller speeds are given in Table 2.

Table 2. Shaft frequency and blades frequency at different impeller speeds.

Variable	Frequency/kHz				
	3000 rpm	2500 rpm	2000 rpm	1500 rpm	1000 rpm
f_n	0.05	0.042	0.033	0.025	0.017
f_{BPF}	0.4	0.333	0.267	0.2	0.133

To obtain frequency domain curves of pressure pulsation at different impeller speeds, pressure pulsation data of monitoring point p1 were transformed by FFT [39–41]. Table 3 shows the dominant frequency of pressure pulsation obtained at different impeller speeds. It can be seen that the dominant frequencies at each impeller speed are distributed in the shaft frequency and multiple blade frequency. For the pump with a single-tongue volute, the dominant frequency of pressure pulsation is blade frequency when the impeller rotates at 3000, 2500, 2000, and 1500 rpm. When the impeller speed is 1000 rpm, the dominant frequency turns to shaft frequency, and the dominant frequency decreases with the decrease of impeller speed. For the pump with the double-tongue volute, the dominant frequency is concentrated at twice the blade frequency when the impeller rotates at 3000 and 2500 rpm. When the impeller speeds are 2000, 1500, and 1000 rpm, the dominant frequency is double-blade frequency, triple-blade frequency, and shaft frequency, respectively.

Table 3. Dominant frequency of pressure pulsation at different impeller speeds.

Volute Condition	Frequency/kHz				
	3000 rpm	2500 rpm	2000 rpm	1500 rpm	1000 rpm
Single-tongue volute	0.396	0.339	0.265	0.024	0.016
Double-tongue volute (static)	0.791	0.662	0.793	0.199	0.016
Double-tongue volute (rotate)	0.784	0.658	0.793	0.198	0.016

Figure 11 shows the frequency domain variation of pressure pulsation at p1 for three volutes at different impellers speeds. By comparing (a) with (b) in Figure 11, it is clear that the dominant frequency of the double-tongue volute at different impeller speeds is higher than that of the single-tongue volute. In addition, the amplitude range of the double-tongue volute is obviously larger than that of the single-tongue volute. This is because, compared with the single-tongue volute, the double-tongue volute has two symmetrical chambers, and the flow pattern becomes more complex, which causes the pressure pulsation of the flow field more violent. As shown in Figure 11b,c, we can find that the frequency domain variation of the rotating double-tongue volute under the same impeller speeds has little difference to that of the static double-tongue volute.

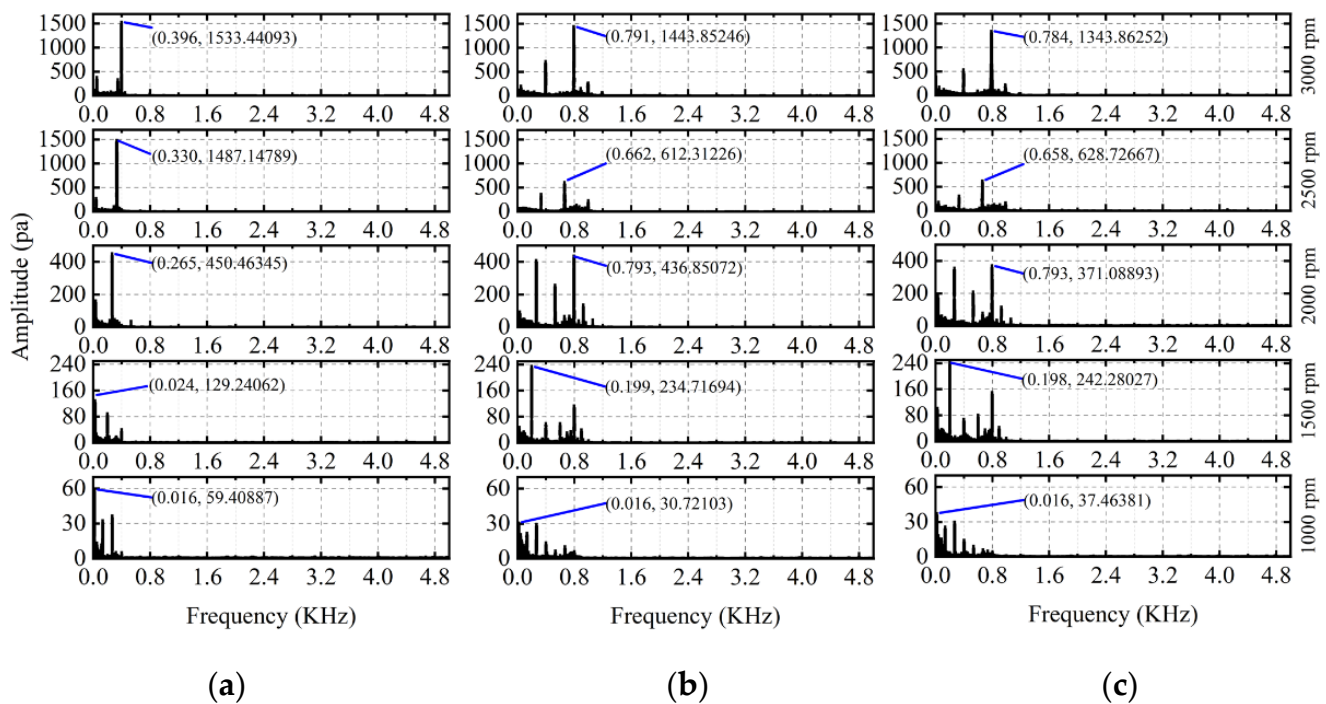


Figure 11. Frequency domain of pressure pulsation for three volutes at different impeller speeds. (a) Single-tongue volute; (b) double-tongue volute (static); (c) double-tongue volute (rotate).

4.2.3. Dominant Frequency Amplitudes of the Pressure Pulsation

The dominant frequency amplitudes of the pressure pulsation are carried out to evaluate the pressure pulsation test to explore the influence of the impeller speeds on the pressure pulsation in the dishwasher pump. Figure 12 shows the dominant frequency amplitudes of the pressure pulsation at different speeds in the pump with three different volutes' conditions. The amplitude of dominant frequency of pressure pulsation of three different volutes decreases with the decrease of impeller speeds. This is because reducing the speed of the impeller makes the pressure of the impeller on the flow decrease and the energy of the pressure pulsation decrease. Compared with the double-tongue volute, when the impeller speed is greater than 2500 rpm, the amplitude of the dominant frequency of the pressure pulsation is not obvious. When the impeller speed is 3000 rpm, the amplitude of the single-tongue volute increases by only 3%, and the amplitude of the double-tongue volute increases by 57% and 53%, respectively, when it is static and rotating. This is because the design flow rate of the double-tongue volute is higher than that of the single-tongue volute at the same impeller speed, and the dishwasher uses an open pump. When the impeller speed is greater than the critical speed, the water will leak out from the impeller outlet and the volute connection. The dishwasher uses an open pump. When the impeller speed is greater than the critical speed, the water flow will leak out from the impeller outlet and the volute connection, which makes the pressure in the pump not change greatly.

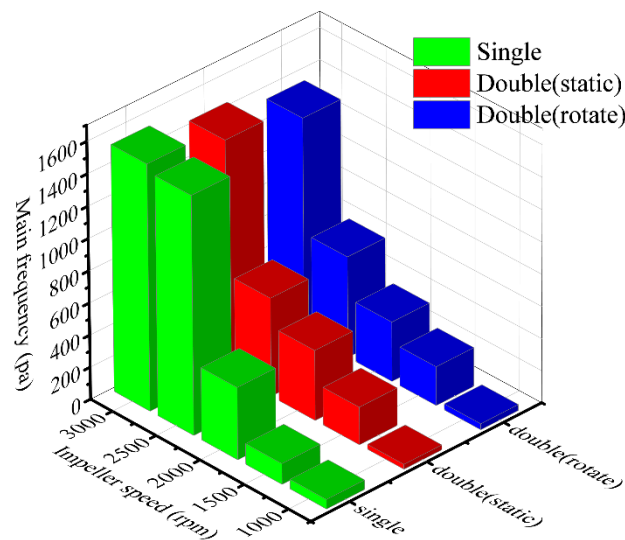


Figure 12. Dominant frequency amplitudes of pressure pulsation for three volutes at different impeller speeds.

5. Conclusions

Experimental tests were carried out to analyze the effects of the single-tongue volute, the static double-tongue volute, and the rotating double-tongue volute on the pressure pulsation characteristics of the dishwasher pump. The pressure pulsation characteristics caused by rotor–stator interference and rotor–rotor interference of the dishwasher pump were analyzed by time domain analysis, frequency domain analysis, and time–frequency domain analysis.

- (1) Compared with the single-tongue volute and the static double-tongue volute, the average pressure of each monitoring point in the dishwasher pump with a rotating double-tongue volute is the smallest, and from the pressure monitoring point from p3 to p6, the average pressure changes more gently, and the maximum deviation value is only 1.4%. The amplitude of the main frequency of the pressure pulsation of the double-tongue volute increases first and then decreases from the monitoring point p1 to p6 and reaches the maximum at the monitoring point p2. However, the amplitude of the main frequency of the single-tongue volute changes irregularly, and the maximum amplitude appears at the monitoring point p1. Therefore, for the dishwasher, the volute with the passive rotation has the best results, which can not only reduce the pressure and reduce vibration noise but also perform all-around cleaning, improving dishwasher efficiency.
- (2) When the impeller rotates at 3000 rpm, the number of peaks and valleys of the pressure pulsation time domain curve of the single-tongue volute is eight, while that of the double-tongue volute is two. The main frequency of the single-tongue volute is 0.396 kHz, which is concentrated near the blade frequency. The main frequencies of the static double-tongue volute and the rotating double-tongue volute are 0.791 kHz and 0.786, respectively, which are concentrated near the double-blade frequency.
- (3) Under the high impeller speeds of 2000, 2500, and 3000 rpm, the pressure pulsation time domain curves present periodicity, and the main frequencies are given priority with the blade frequency and integer times of the blade frequency. At the low impeller speeds of 1000 and 1500 rpm, the pressure pulsation becomes disordered, the periodicity of the time-domain curves disappears, and the main frequency is mainly axial frequency.

Author Contributions: Writing—draft preparation, Y.Z.; writing—review and editing, Y.L.; methodology, Y.L.; software, J.Z.; conceptualization, J.Z. and Y.L.; formal analysis, J.Z. and Y.L.; funding acquisition, J.Z. and Y.L.; project administration, H.X. and F.Z.; supervision, P.H., H.X. and F.Z. All authors have read and agreed to the published version of the manuscript.

Funding: This work is supported by the project of National Natural Science Foundation of China (No. 51809120), the Natural Science Foundation of Jiangsu Province (No. BK20180871), the Project Funded by China Postdoctoral Science Foundation (No. 2018M640462), the Natural Science Foundation of the Jiangsu Higher Education Institutions of China (No. 18KJB470005), the Key Research and Development Plan Project of Jiangsu Province (No. BE2019009), and A Project Funded by the Priority Academic Program Development of Jiangsu Higher Education Institutions (PAPD).

Institutional Review Board Statement: Not applicable.

Informed Consent Statement: Not applicable.

Data Availability Statement: Not applicable.

Conflicts of Interest: The authors declare no conflict of interest.

References

1. Zhang, L.; Wang, C.; Zhang, Y.C. Numerical study of coupled flow in blocking pulsed jet on a rotating wall. *J. Braz. Soc. Mech. Sci.* **2021**, *43*, 508. [\[CrossRef\]](#)
2. Wang, H.L.; Qian, Z.D.; Zhang, D. Numerical study of the normal impinging water jet at different impinging height, based on Wray–Agarwal turbulence model. *Energies* **2020**, *13*, 1744. [\[CrossRef\]](#)
3. Li, D.Y.; Wang, H.J.; Qin, Y.L. Numerical simulation of hysteresis characteristic in the hump region of a pump-turbine model. *Renew. Energy* **2018**, *115*, 438–447. [\[CrossRef\]](#)
4. Li, D.Y.; Wang, H.J.; Qin, Y.L. Mechanism of high amplitude low frequency fluctuations in a pump-turbine in pump mode. *J. Mech. Sci. Technol.* **2018**, *126*, 668–680. [\[CrossRef\]](#)
5. Xia, L.S.; Cheng, Y.G.; Cai, F. Pressure pulsation characteristics of a model pump-turbine operating in the S-shaped region: CFD simulations. *Int. J. Fluid Mach. Syst.* **2017**, *10*, 287–295. [\[CrossRef\]](#)
6. Tang, S.N.; Zhu, Y.; Yuan, S.Q. An improved convolutional neural network with an adaptable learning rate towards multi-signal fault diagnosis of hydraulic piston pump. *Adv. Eng. Inform.* **2021**, *50*, 101406. [\[CrossRef\]](#)
7. Zhu, Y.; Li, G.P.; Wang, R. Intelligent fault diagnosis of hydraulic piston pump combining improved LeNet-5 and PSO hyperparameter optimization. *Appl. Acoust.* **2021**, *183*, 108336. [\[CrossRef\]](#)
8. Jin, J.M.; Jung, K.J.; Kim, Y.H. Effects of gap between impeller and volute tongue on a pressure fluctuation in double-suction pump. *J. Mech. Sci. Technol.* **2020**, *34*, 4879–4903. [\[CrossRef\]](#)
9. Alemi, H.; Nourbakhsh, S.A.; Raisee, M. Effect of the volute tongue profile on the performance of a low specific speed centrifugal pump. *Proc. Inst. Mech. Eng. Part A J. Power Energy* **2015**, *229*, 210–220. [\[CrossRef\]](#)
10. Patil, S.R.; Chavab, S.T.; Jadhav, N.S. Effect of volute tongue clearance variation on performance of centrifugal blower by numerical and experimental analysis. *Mater. Today* **2018**, *5*, 3883–3894. [\[CrossRef\]](#)
11. Shim, H.S.; Afzal, A.; Kim, K.Y. Three-objective optimization of a centrifugal pump with double volute to minimize radial thrust at off-design conditions. *Proc. Inst. Mech. Eng. Part A J. Power Energy* **2016**, *230*, 598–615. [\[CrossRef\]](#)
12. Yang, S.H.; Kong, F.Y.; Chen, B. Research on pump volute design method using CFD. *Int. J. Rotating Mach.* **2011**, *2011*, 137860. [\[CrossRef\]](#)
13. Wang, H.L.; Long, B.; Wang, C. Effects of the impeller blade with a slot structure on the centrifugal pump performance. *Energies* **2020**, *13*, 1628. [\[CrossRef\]](#)
14. Zhou, J.R.; Zhao, M.M.; Wang, C. Optimal design of diversion piers of lateral intake pumping station based on orthogonal test. *Shock Vib.* **2021**, *2021*, 6616456. [\[CrossRef\]](#)
15. Wang, H.L.; Hu, Q.X.; Yang, Y. Performance differences of electrical submersible pump under variable speed schemes. *Int. J. Simul. Model.* **2021**, *20*, 76–86. [\[CrossRef\]](#)
16. Shi, L.J.; Zhu, J.; Tang, F.P. Multi-Disciplinary optimization design of axial-flow pump impellers based on the approximation model. *Energies* **2020**, *13*, 779. [\[CrossRef\]](#)
17. Li, Q.Q.; Li, S.Y.; Wu, P. Investigation on reduction of pressure fluctuation for a double-suction centrifugal pump. *Chin. J. Mech. Eng.* **2021**, *34*, 192–209. [\[CrossRef\]](#)
18. Zhang, J.F.; Appiah, D.; Zhang, F. Experimental and numerical investigations on pressure pulsation in a pump mode operation of a pump as turbine. *Energy Sci. Eng.* **2019**, *7*, 1264–1279. [\[CrossRef\]](#)
19. Tan, L.; Yu, Z.Y.; Xu, Y. Role of blade rotational angle on energy performance and pressure fluctuation of a mixed-flow pump. *Proc. Inst. Mech. Eng. Part A J. Power Energy* **2017**, *231*, 227–238.
20. Meng, L.; Zhang, S.P.; Zhou, L.J. Study on the pressure pulsation inside runner with splitter blades in ultra-high head turbine. *IOP Conf. Ser. EES* **2014**, *22*, 032012. [\[CrossRef\]](#)

21. Xia, L.S.; Cheng, Y.G.; Zhang, X.X. Numerical analysis of rotating stall instabilities of a pump- turbine in pump mode. *IOP Conf. Ser. EES* **2014**, *22*, 032020. [[CrossRef](#)]
22. Wu, D.H.; Ren, Y.; Mou, J.G. Investigation of pressure pulsations and flow instabilities in a centrifugal pump at part-load conditions. *Int. J. Fluid Mach. Syst.* **2017**, *10*, 355–362. [[CrossRef](#)]
23. Shi, L.J.; Yuan, Y.; Jiao, H.F. Numerical investigation and experiment on pressure pulsation characteristics in a full tubular pump. *Renew. Energy* **2021**, *163*, 987–1000. [[CrossRef](#)]
24. Zhang, F.; Lowys, P.Y.; Houdeline, J.B. Pump-turbine rotor-stator interaction induced vibration: Problem resolution and experience. *IOP Conf. Ser. EES* **2021**, *774*, 012124. [[CrossRef](#)]
25. Song, X.J.; Liu, C. Experimental investigation of pressure pulsation induced by the floor-attached vortex in an axial flow pump. *Adv. Mech. Eng.* **2019**, *11*, 1–13. [[CrossRef](#)]
26. Liu, Y.P.; Li, X.J.; Li, B.W. Influence of impeller sinusoidal tubercle trailing-edge on pressure pulsation in a centrifugal pump at nominal flow rate. *J. Fluids Eng.* **2021**, *143*, 091205.
27. Duan, X.H.; Tang, F.P.; Duan, W.Y.; Zhou, W.; Shi, L. Experimental investigation on the correlation of pressure pulsation and vibration of axial flow pump. *Adv. Mech. Eng.* **2019**, *11*, 1–11. [[CrossRef](#)]
28. Ni, D.; Zhang, N.; Gao, B. Dynamic measurements on unsteady pressure pulsations and flow distributions in a nuclear reactor coolant pump. *Energy* **2020**, *198*, 117305. [[CrossRef](#)]
29. Zhang, N.; Yang, M.G.; Gao, B. Experimental and numerical analysis of unsteady pressure pulsation in a centrifugal pump with slope volute. *J. Mech. Sci. Technol.* **2015**, *29*, 4231–4238. [[CrossRef](#)]
30. Wang, W.J.; Pei, J.; Yuan, S.Q. Experimental investigation on clocking effect of vaned diffuser on performance characteristics and pressure pulsations in a centrifugal pump. *Energy* **2018**, *90*, 286–298. [[CrossRef](#)]
31. Allen, J.B. Short term spectral analysis, synthesis, and modification by discrete Fourier transform. *IEEE Trans. Acoust. Speech Signal Process.* **1977**, *25*, 235–238. [[CrossRef](#)]
32. Sun, T.Z.; Zhang, X.S.; Zhang, J.Y. Experimental study on the unsteady natural cloud cavities: Influence of cavitation number on cavity evolution and pressure pulsations. *J. Mar. Sci. Eng.* **2021**, *9*, 1–13. [[CrossRef](#)]
33. Wang, C.; Zhang, Y.X.; Li, Z.W. Pressure fluctuation–vortex interaction in an ultra-low specific-speed centrifugal pump. *J. Low Freq. Noise Vib. Act. Control.* **2019**, *38*, 527–543. [[CrossRef](#)]
34. Bai, L.; Zhou, L.; Han, C.; Zhu, Y.; Shi, W. Numerical study of pressure fluctuation and unsteady flow in a centrifugal pump. *Processes* **2019**, *7*, 354. [[CrossRef](#)]
35. Bosioc, A.I.; Tanasa, C.; Muntean, S. Unsteady pressure measurements and numerical investigation of the jet control method in a conical differ with swirling flow. *IOP Conf. Ser. EES* **2010**, *12*, 012017. [[CrossRef](#)]
36. Zhou, Q.; Zhao, X.W.; Pei, L. Investigation on pressure pulsation and modal behavior of the impeller in a nuclear reactor coolant pump. *Energy Sci. Eng.* **2021**, *9*, 1440–1449. [[CrossRef](#)]
37. Yang, J.; Liu, J.; Liu, X.H. Numerical study of pressure pulsation of centrifugal pumps with the compressible mode. *J. Therm. Sci.* **2019**, *28*, 106–114. [[CrossRef](#)]
38. Gao, Y.S.; Cheng, J.; Huang, J.H. Simulation analysis and experiment of variable-displacement asymmetric axial piston pump. *Appl. Sci.* **2017**, *7*, 328. [[CrossRef](#)]
39. Yang, Y.; Zhou, L.; Shi, W.D. Interstage difference of pressure pulsation in a three-stage electrical submersible pump. *J. Petrol. Sci. Eng.* **2021**, *196*, 107683. [[CrossRef](#)]
40. Zhou, Q.; Li, H.K.; Pei, L. Research on non-uniform pressure pulsation of the diffuser in a nuclear reactor coolant pump. *Nucl. Eng. Technol.* **2020**, *53*, 1020–1028. [[CrossRef](#)]
41. Muntean, S.; Tanasa, C.; Bosioc, A.I. Investigation of the plunging pressure pulsation in a swirling flow with precessing vortex rope in a straight diffuser. *IOP Conf. Ser. EES* **2016**, *49*, 082010. [[CrossRef](#)]